論文の内容の要旨

CONDENSATION OF CONFINED EXCITON-POLARITONS AND THEIR EXCITATIONS
(トラップされた励起子ポラリトンの凝縮体と励起状態)

氏名　宇都宮 聖子

Bose-Einstein condensation (BEC) is generally defined as a macroscopic occupation of a single-particle quantum state, a phenomenon often referred to as off-diagonal long-range order due to non-vanishing off-diagonal components of the one-body density. Since the theoretical prediction of BEC in an ideal gas of non-interacting bosons by Einstein in 1925, BEC in dilute atomic gases has been long-waited and finally demonstrated by two experimental groups in 1995. In the past decade, a new solid state system called exciton-polaritons, which are half-matter, half-light quasiparticles in semiconductor microcavities, has attracted considerable attention as a new candidate of Bose Einstein condensate in solid state systems.

Bose-Einstein condensation was theoretically predicted in Einstein's 1925 paper, based upon the Bose's statistical description of quanta of light in 1924. However, Einstein's prediction had been neglected for more than ten years, since BEC was regarded as not much more than a theoretical anecdote. The discovery of superfluidity in liquid ^{4}He by Kapitza and by Allen and Misener in 1938 stimulated the interest in BEC physics. The hypothesis of the connection between superfluidity and BEC by London motivated the theoretical study of BEC. Shortly after that, Tisza used the notion of BEC in his two-fluid hydrodynamics model in 1938, which describes the co-existence of thermal and condensate phases in the fluid. In 1941, Landau noticed that liquid could be described in terms of weakly interacting particles rather than non-interacting particles. This phenomenological description of a superfluid assumes a relatively simple excitation energy spectrum for two kinds of quasiparticles: phonons and rotons. A quantum field-theoretical formulation by Bogoliubov in 1947 established a microscopic theory for weakly interacting Bose gases, which yielded directly the phonon-like excitation spectrum. Cohen and Feynman suggested that the excitation spectrum could be observed by thermal neutron scattering experiments. However, the observed excitation spectrum agreed only qualitatively due to strong particle-particle interaction of liquid helium. In 1995, the experimental group of Cornel and Wieman at Boulder and that of Ketterle at MIT succeeded in reaching critical temperatures and densities required to

observe BEC in dilute atomic gases with different cooling techniques. Experimental verification of the Bogoliubov theory only came with that long-waited BEC of weakly interacting particles.

The exciton-polariton in a semiconductor microcavity is a promising solid state system for studying the dynamical condensation phenomena in solids. Since its effective mass is eight orders of magnitude smaller than the atomic hydrogen mass and four orders of magnitude lighter than the exciton mass, the critical temperature of polariton BEC transition is expected to be up to room temperature. Furthermore the experimental set up is rather compact and simple compared to that of cold atoms or liquid helium. Meanwhile, the exciton BEC was theoretically predicted in 1965, but it has never realized because of notorious problems inherent to solid state systems, that is a relatively short lifetime, dissociation of excitons at high densities by screening, Auger recombination and phase space filling and localization of excitons due to disorder and inhomogeneous potential.

Recent experimental progress with exciton polaritons demonstrated several promising signatures for polariton condensation, such as quantum degeneracy at nonequilibrium condition, polariton bunching effect at condensation threshold, long spatial coherence and finally quantum degeneracy at equilibrium condition. Those experimental results are good smoking guns but not sufficient to convince the scientific community with the occurrence of BEC. This is mainly because the exciton-polariton system is a dynamical system due to its short lifetime and a complicated system due to its solid state environment.

The particle-particle interaction, which is in the intermediate coupling regime between strongly interacting superfluid ^{4}He and weakly interacting dilute atomic gas in the case of polariton, and peculiar excitation spectra are keys for understanding BEC and superfluidity. In this thesis the five distinct signatures of the polariton-polariton interaction are studied: In this thesis the five distinct signatures of the polariton-polariton interaction are studied: (1) blue shift of the condensate energy U due to repulsive interaction among condensate polaritons (Fig. 1), (2) expanding condensate size with polariton density due to the same origin (Fig. 2), (3) increasing position-momentum uncertainty product to above the Heisenberg limit (Fig. 2), (4) phonon-like dispersion of excitations at small momentum region (Fig. 3) and (5) blue shift of particle-like excitation energy $2U$ at large momentum regime due to the

interaction between the condensate and thermally excited particles (Fig. 4).

For the observation of BEC, we used circular traps to induce the effective potential barrier for polaritons by depositing the thin metal film, which modulate the effective photon field in a microcavity and increase a resonant energy of a cavity photon field and also lower polariton energy. When energetic polaritons are injected near a trap, those polaritons are cooled by collision with lattice and eventually confined in a trap made of a hole of metal film, where the lower polariton energy is ~200μeV lower than that in the surrounding area. Trapped polaritons condense into nearly a single-transverse mode and features a position-momentum uncertainty product close to the Heisenberg limit.

We showed the quantitative agreement of Bogoliubov theory and experimentally observed excitation spectra which stem from the condensate of polaritons in traps in Fig. 3 and 5. In Fig. 5, we confirmed that excitation spectra of trapped polariton condensate agrees with inhomogeneous and homogeneous model of Bogoliubov excitation near $|k\xi|=1$ at different densities. In both the phonon-like regime $|k\xi|<1$ and the free particle regime at $|k\xi|>1$, the experimental results agree well with the universal curve in Fig. 3. We also investigated polarization dependence of condensation and excitation spectra and confirmed the excitation part has the same polarization as the condensate.

As for the first important experimental result in this thesis, for the observation of condensate, we showed the quantitative agreement of Bogoliubov theory and experimentally observed excitation spectra which stem from the condensate of polaritons in traps. In both the phonon-like regime $|k\zeta|<1$ and the free particle regime at $|k\zeta|>1$, the experimental results agree well with the universal curve. We also investigated polarization dependence of condensation and excitation spectra and confirmed the excitation part has the same polarization as the condensate.

As the second important result is that we observed that 1D arrayed polariton shows the condensates spectra, which is normally obtained at the ground state energy, at excited state energy with "π-phase" modulation between adjacent sites. The wave function of the condensate plays a role as an order parameter, whose phase is essential in characterizing the coherence and superfluid phenomena. The long-range spatial coherence leads to the existence of phase-locked multiple condensates in an array of superfluid helium, superconducting Josephson junctions, or atomic BECs. Under certain circumstances, a quantum phase difference of π is predicted to develop among

weakly coupled Josephson junctions. Such a meta-stable π-state was discovered in a weak link of superfluid ^{3}He, which is characterized by a 'p-wave' order parameter. Possible existence of such a π-state in weakly coupled atomic BECs has also been proposed, but remains undiscovered. We observed the spontaneous buildup of inphase ('zero-state') and antiphase ('π-state') 'superfluid' states in an exciton-polariton condensate array connected by weak periodic potential barriers as shown in Fig. 6 and 7. These states reflect the band structure of the one-dimensional polariton array and the dynamic characteristics of meta-stable exciton-polariton condensates.

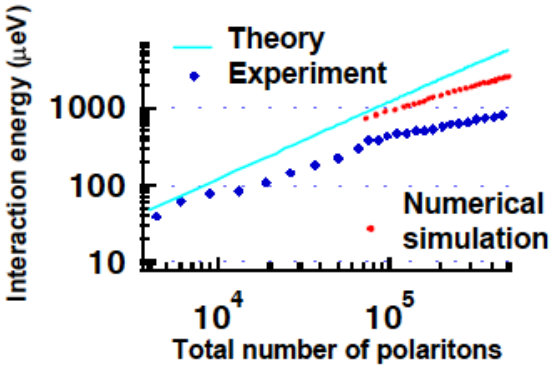

Fig. 1 | The measured LP energy shift at k=0 (blue diamonds) and calculated energy shift $U(n)$ (light blue solid line) are plotted as a function of total number of polaritons. The numerical results by the GP equation, including the effect of pump dependent condensate size, are shown by red dots.

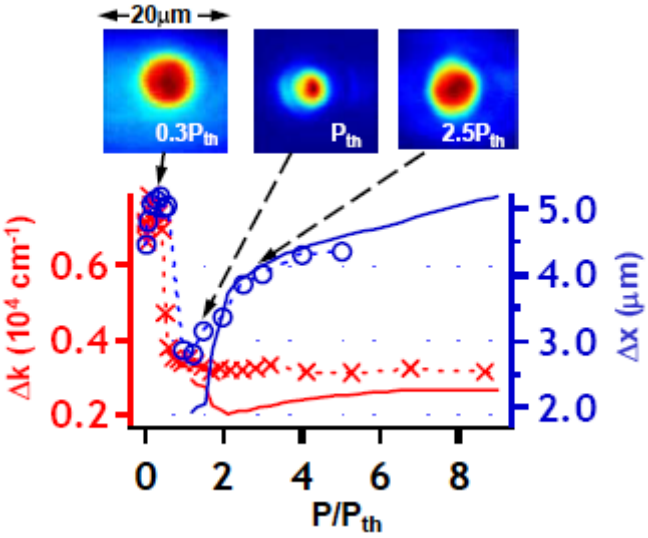

Fig. 2 | The measured standard deviations of LP distribution in coordinate Δx (blue circles) and in wavenumber Δk (red crosses) are plotted as a function of P/P_{th}. Theoretical values for Δx and Δk obtained by the GP equation are shown by blue and red solid lines. Top panels are the near field images at three different pump levels; $0.3P_{th}$, P_{th} and $2.5P_{th}$.

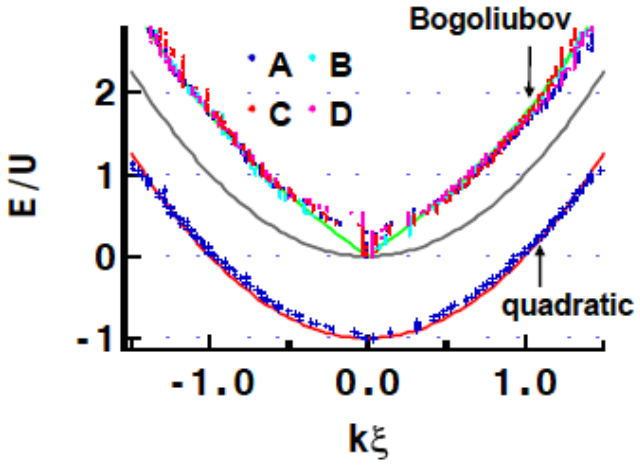

Fig. 3| Numerically searched excitation energy normalized by the interaction energy $E/U(n)$ as a function of normalized wavenumber $k\xi$ for four different untrapped condensate systems. The experimental data far below threshold is also plotted by blue crosses for the system A. Three theoretical dispersion curves normalized by the interaction energy are plotted; the Bogoliubov excitation energy $E_B/U(n)$ starting from the condensate energy (green solid line), the quadratic dispersion curves $E_{LP}^2/U(n)$ (grey solid line) and free polariton dispersion $E_{LP}/U(n)$ (red solid line).

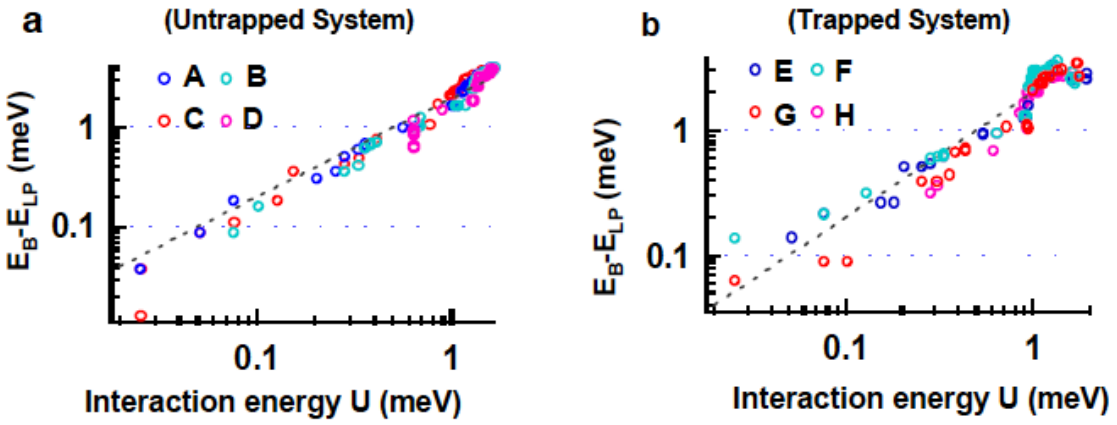

Fig. 4| The energy shift $E_B - E_{LP}$ in the free particle regime ($|k\xi|=1$) is plotted as a

function of the interaction energy $U(n)$ for four different untrapped systems (**a**) and four different trapped systems b).

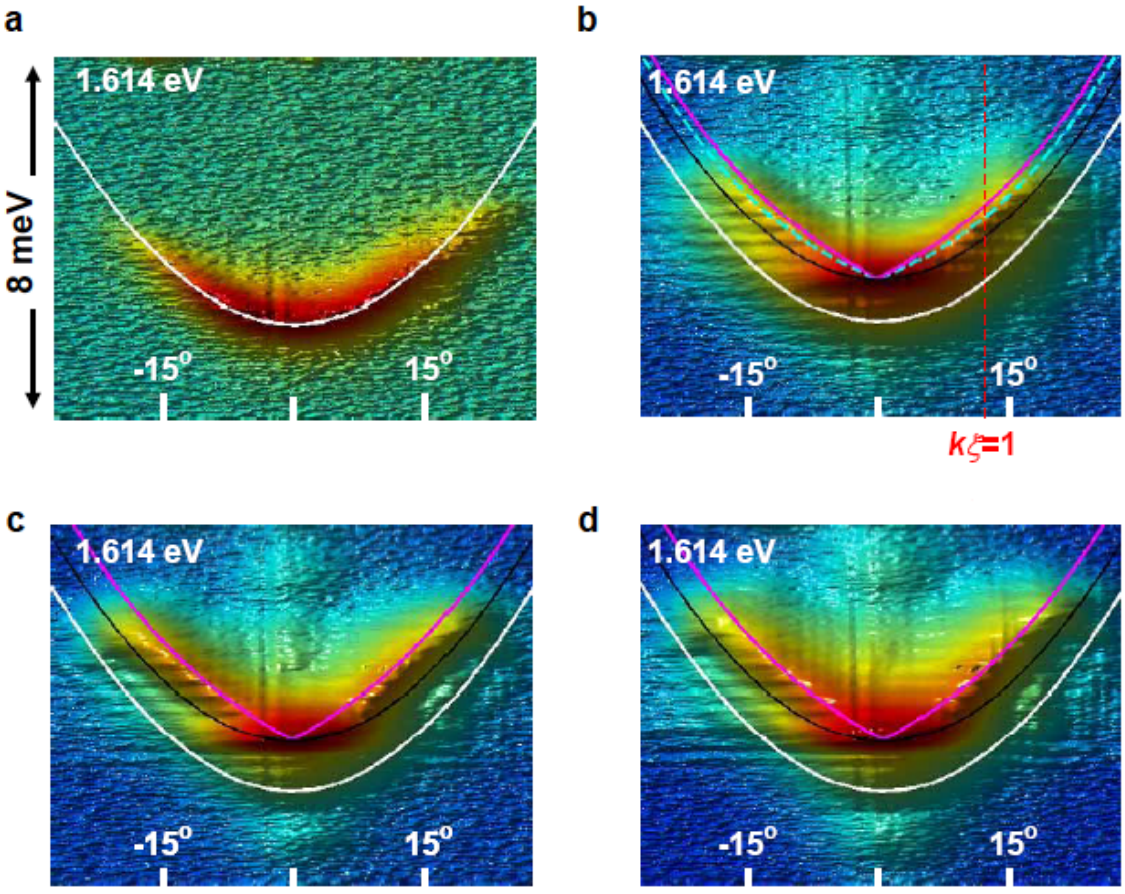

Fig. 5| Time integrated dispersion relations between the LP energy (in the range of 8 meV centered at 1.61 eV) vs. in-plane wavenumber. The circularly polarized pump beam is injected into a trap with 8μm diameter, where the detuning parameter is Δ=1.6 meV. Pump rates are **a:** P=0.05 P_{th}, **b:** P=1.2 P_{th}, **c:** P=4 P_{th} and **d:** P=6 P_{th}, where P_{th} =4mW. Three theoretical curves represent the Bogoliubov excitation energy E_B based on the homogeneous model (pink line), the quadratic dispersion curve $E_{LP'}$ starting from the condensate energy (black line) and the non-interacting free polariton quadratic dispersion curve E_{LP} (white line) that is determined by the experimental data shown in Fig. 3a. In Fig. 3b light blue dotted line shows the Bogoliubov excitation curve based on the local density approximation.

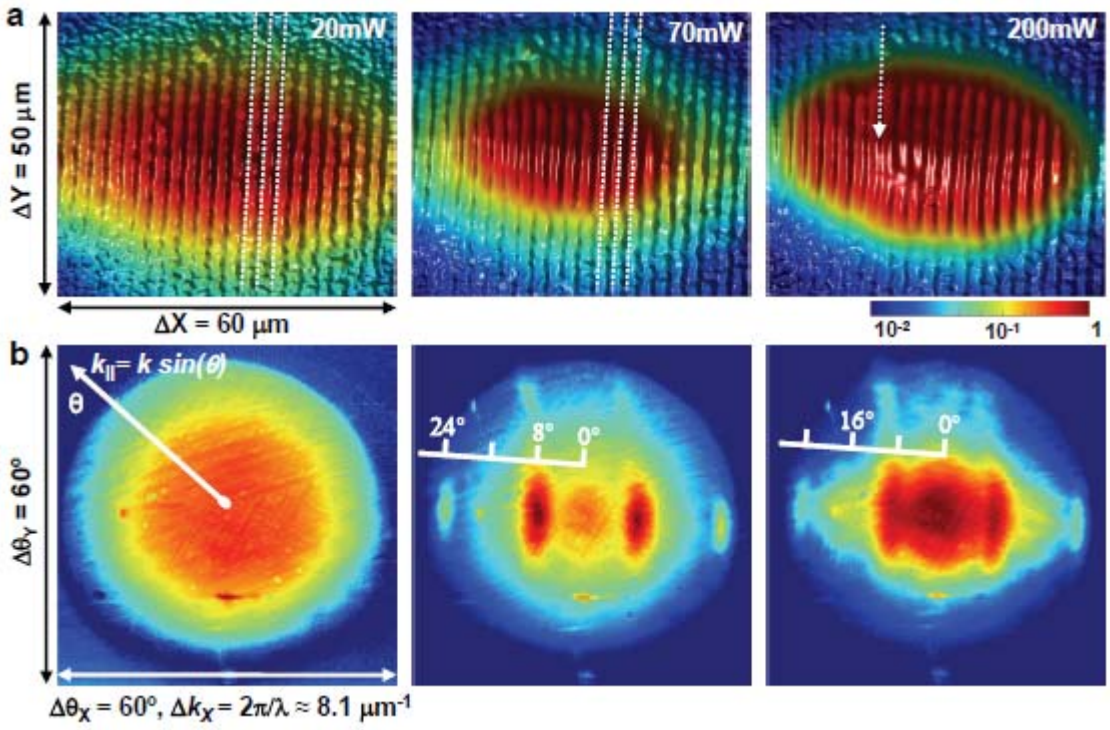

Fig. 6| Imaging and spectroscopy of exciton-polariton distribution in coordinate and momentum space. a, Near-field images showing the LP distribution across a polariton array in coordinate space under pumping powers of 20, 70, and 200 mW (left to right). The threshold pumping power is about 45 mW. The elliptical pumping spot covers approximately 20 periodic elements. The white dashed lines indicate locations on the metal film, where LP emissions are minimal in these locations due to the attenuation by metal strips. The offset observed at the boundary between the condensate and the non-condensate for 70 mW indicates that dominant emissions are from the metallic strips in spite of the attenuation. This result suggests the effective Bloch wavefunction for the condensate is 'p-state'. Under higher pumping rates, the near-field image of the condensate recovers a standard spatial modulation (corresponding to the 's-state' condensate; near the central area indicated by the white arrow). **b.** Corresponding far-field images showing the LP distribution in momentum space. When passing through the threshold, lobes at ~±8º and ~±24º emerges out of the isotropic background of the thermal polariton gas, which is indicative of the 'π-state'. The strong central lobe at 0º and two weak lobes at ~±16º appear at higher pumping rates, indicative of the 'zero-state'. The sample is held at T = 20 K for this set of measurements.

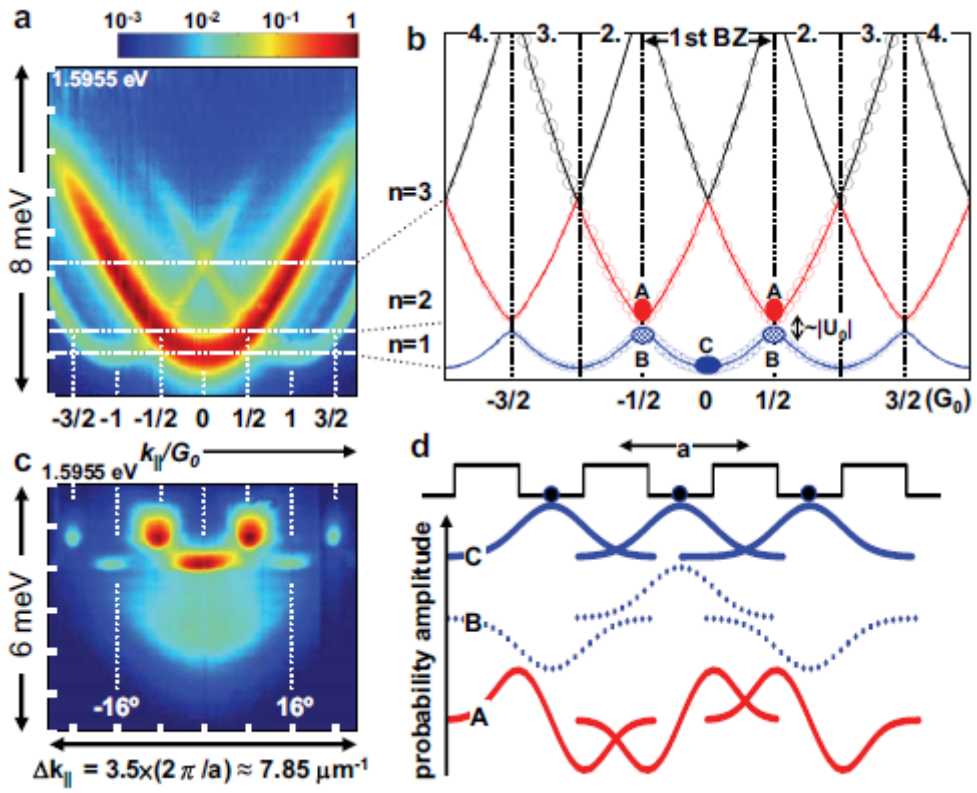

Fig. 7| Band structure and 'superfluid' states in an exciton-polariton condensate array. a, Time-integrated energy versus in-plane momentum of an exciton-polariton array at near resonance $E_C \approx E_X$. The pumping power is P = 10 mW (below threshold). The central bright parabola corresponds to the dispersion curve for the polaritons in the absence of a periodic potential. Two additional parabolas (intensity ~5% of the central one) displaced by $\pm G_0 = \pm 2\pi / a$ cross the central dispersion curve at $k_{\|} = 0, \pm G_0 / 2$. **b,** Extended-zone scheme of the band structure for the exciton-polariton array under a weak periodic potential with a lattice constant *a*. Anti-crossing occurs at the boundary between the 1st and 2nd Brillouin zones (BZ). The size of open circles represents the expected relative emission intensity (log scale) of each energy band. Condensation occurs at the valleys labeled by solid red (point A) and blue (point C) circles. **c,** Energy versus in-plane momentum of an exciton-polariton condensate array at blue detuning $E_C - E_X \approx 6$ meV above threshold (P = 40 mW). The lobes at $k_{\|} = 0, \pm G_0$ correspond to the inphase 'zero-state', whereas the lobes at $k_{\|} = \pm G_0 / 2, \pm 3G_0 / 2$ correspond to the antiphase 'π-state'. The energy difference between two states is about 0.7 meV, equal to energy difference between the first anticrossings (point A) and the bottom of the dispersion parabola (point C). **d,** Schematic

illustrations of the Bloch wave functions for states labeled as A, B, C in (b). The meta-stable condensate at point A consists of ‘p-states’ connected by π-phase difference, while the ground state condensate at point C consists of ‘s-states’ connected by zero-phase difference.